

## Analysis of charge-dependent stopping of swift ions

Peter Sigmund

*Fysisk Institut, Odense Universitet, DK-5230 Odense M, Denmark\**  
*and Institut de Physique Nucléaire, Université Paris-Sud, F-91406 Orsay, France*  
 (Received 18 February 1994; revised manuscript received 8 June 1994)

Rigorous expressions have been derived for the mean energy loss of ions penetrating through foils, specified into entrance and exit charge states. These expressions allow extraction of partial stopping cross sections and charge-exchange cross sections in solids from measured energy losses versus foil thickness. Particular attention is given to thin penetrated layers and the opposite limit of charge-state equilibrium which may be easier to deal with experimentally. Sum rules to be obeyed by measured parameters have been derived. Explicit results have been listed for the two-state case.

PACS numbers: 34.50.Bw, 52.40.Mj, 61.80.Mk

### I. INTRODUCTION

It is well known that the stopping of an ion in matter depends on its charge state [1]. Allison and co-workers [2] reported systematic measurements on keV hydrogen and helium beams penetrating through gas targets thin enough so that at most one charge-changing event could affect the measurements significantly. The quantity emerging from such measurements is an  $n \times n$  matrix of partial stopping sections, where  $n$  is the number of accessible states. Datz *et al.* [3] and later Golovchenko *et al.* [4] performed similar measurements on heavier ions traveling through crystals under channeling conditions, utilizing the observation of frozen charge states in the absence of violent collisions. Cowern and co-workers [5] analyzed the stopping of swift heavy ions in amorphous foils under conditions where charge-changing events were more frequent. Ogawa and co-workers [6] reported measurements employing MeV helium on carbon foils under conditions where only two charge states were involved and where the number of charge-changing events was small.

The present paper addresses the problem of a systematic analysis of experimental data on entrance- and exit-state-dependent energy loss, with the aim of determining atomic parameters that might be difficult to find experimentally by other means, in particular for penetration through solid matter. In principle, an  $n \times n$  matrix of energy-loss spectra can be measured for a range of incident energies and target thicknesses. This should provide direct information on parameters governing the pertinent events on an atomic scale.

In the absence of charge-changing events, i.e., for very thin penetrated layers, mainly the collisional stopping cross section is determined for each incident state. Experiments on thicker targets have commonly been analyzed by Winterbon's scheme [7,8] or by Monte Carlo simulation. While the former is elegant, it invokes a couple of

simplifying assumptions that are not necessarily fulfilled: The loss spectrum in an individual event was taken to be Coulomb-like and  $\propto q^2$ ,  $q$  being the ionic charge; more important, energy loss in charge-changing events was ignored. Monte Carlo simulations allow incorporation of all pertinent effects, but the choice of physically acceptable input among a wide variety of conceivable parameters is a notorious problem in the fitting procedure. The scheme employed in Ref. [6] is limited to thin penetrated layers since it does not allow for more than one charge-changing event.

### II. QUALITATIVE CONSIDERATIONS

Figure 1 shows a schematic view of the mean rate of energy loss of an impinging ion on the penetrated depth. Transients are observed if the incident charge state deviates from equilibrium. The magnitude of the deviation of the stopping power from its equilibrium value is governed by its dependence on charge state, and the approach to equilibrium is governed by the pertinent cross sections for electron capture and loss.

In experiments with ion beams penetrating solid foils at moderate speed, the range of accessible foil thicknesses may allow only measurements near or at charge-state equilibrium. Therefore it may be difficult to impossible to determine cross sections for charge exchange by direct measurements like those that are standard for gaseous targets.

Figure 2 shows the dependence of the mean energy loss of an ion on foil thickness for a situation like that sketched in Fig. 1. It is seen that the transient behavior manifests itself in an intercept of the asymptotically linear dependence of energy loss on foil thickness. The magnitude of such intercepts can be measured even on thick targets where the charge state has equilibrated. In other words, the mean energy loss carries a memory of the transient behavior. The actual number of measurable intercepts depends on the number of charge states involved. Clearly, information on charge-exchange cross sections as well as the dependence of stopping power on

\*Permanent address.

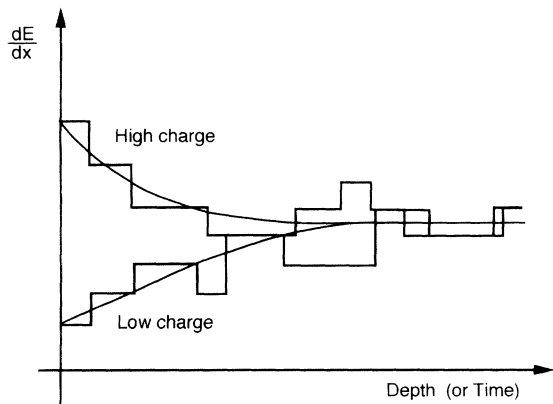


FIG. 1. Schematic view of the depth dependence of the mean rate of energy loss of a penetrating ion.

charge state may be gained if a suitable method of analysis is available. To the author's knowledge, no general formalism has been provided in the existing literature that would explicitly link these intercepts to pertinent atomic parameters.

The dependence on entrance state sketched in Figs. 1 and 2 must have its equivalent on the exit side: Indeed, an ion emerging in a high charge state must have experienced an exceptionally high rate of energy loss near exit, and vice versa. Therefore measurements of the mean energy loss for different exit states must provide a second set of intercepts containing complementary information to that found on entrance.

### III. BASIC EQUATIONS

A general expression for the energy-loss spectrum dependent on entrance and exit state has been found recently [9,10]. In the absence of spontaneous events such as Auger transitions, the well-known Bothe-Landau integral turns into a matrix

$$\mathbf{F}(\Delta E, x) = \frac{1}{2\pi} \int_{-\infty}^{\infty} dk e^{ik\Delta E} e^{N\mathbf{x}[\mathbf{Q} - \boldsymbol{\sigma}(k)]} \quad (1)$$

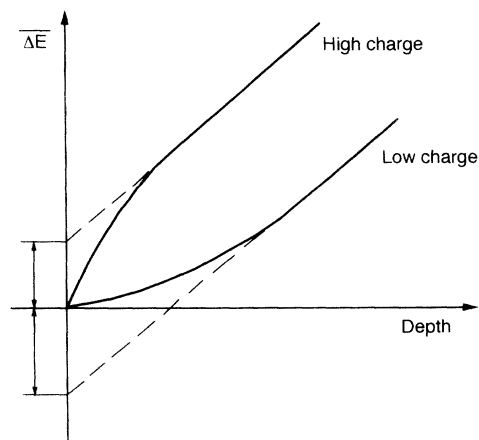


FIG. 2. Schematic view of the dependence on target thickness of the mean energy loss of a penetrating ion.

with the elements  $F_{IJ}(\Delta E, x)$ , where the row index denotes the entrance and the column index the exit state of the ion,  $\Delta E$  the energy loss,  $x$  the target thickness, and  $N$  the number density of the material. The matrix  $\boldsymbol{\sigma}(k)$  has the elements  $\sigma_{IJ}(k) = \int d\sigma_{IJ}(T) (1 - e^{-ikT})$ , where  $d\sigma_{IJ}(T)$  is the differential cross section for energy loss  $(T, dT)$  and simultaneous switch from state  $I$  to  $J$ . The matrix  $\mathbf{Q}$  has the elements  $Q_{IJ} = \sigma_{IJ} - \delta_{IJ} \sum_K \sigma_{IK}$ , where  $\sigma_{IJ}$  is the total cross section (regardless of energy loss) for a transition from state  $I$  to  $J$ , and  $\delta_{IJ}$  is the Kronecker symbol.

The development of the charge-state population with layer thickness  $x$  is described by a matrix  $\mathbf{F}(x)$  with the elements

$$F_{IJ}(x) = (e^{N\mathbf{x}\mathbf{Q}})_{IJ}, \quad (2)$$

as is easily verified by integration of Eq. (1) over all exit energies. Equations (1) and (2) hinge on two assumptions: (i) statistical independence of individual collision and/or charge-changing events; (ii) total energy loss small enough so that all variation of pertinent cross sections across the layer thickness can be neglected.

The present analysis focuses on the mean energy loss

$$\begin{aligned} \langle \Delta E \rangle_{IJ} &= \frac{1}{F_{IJ}(x)} \int d(\Delta E) \Delta E F_{IJ}(\Delta E, x) \\ &= \frac{1}{F_{IJ}(x)} N \int_0^x dx' [\mathbf{F}(x') \cdot \mathbf{S} \cdot \mathbf{F}(x - x')]_{IJ}, \end{aligned} \quad (3)$$

where  $\mathbf{S}$  is a matrix with the elements  $S_{KL} = \int T d\sigma_{KL}(T)$  which denote stopping cross sections for individual collisions involving initial and final state  $K$  and  $L$ , respectively. Diagonal elements  $S_{KK}$  represent "collisional energy loss" in state  $K$ ; off-diagonal elements reflect the contribution to stopping from charge-changing events.

Figure 3 illustrates the origin of the expression in the last identity of Eq. (3). Consider the mean energy loss of a projectile to a layer of thickness  $dx'$  at depth  $x'$ . The probability for the projectile to occupy some state  $K$  at this depth is  $F_{IK}(x')$ . The mean energy loss in the layer is  $Ndx'S_{KL}$  for a collision resulting in a switch to state

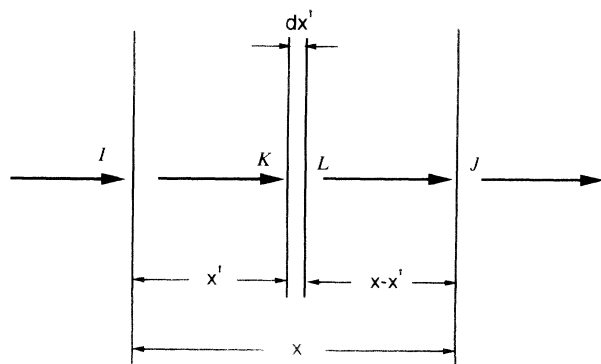


FIG. 3. Direct derivation of Eq. (3). See text.

$L$ , the case of  $L = K$  being allowed for. The probability for the ion thereafter to emerge in state  $J$  at the foil thickness  $x$  is  $F_{LJ}(x - x')$ . The mean energy loss  $\langle \Delta E \rangle_{IJ}$  is found by summation over all intermediate states  $K$  and  $L$ , integration over all layers  $dx'$ , and division by the overall probability  $F_{IJ}(x)$  for emerging in state  $J$ .

#### IV. EXPANSIONS

Equations (2) and (3) need to be customized to be applicable in practice. In the following, two important lim-

$$\langle \Delta E \rangle_{IJ} = Nx \left[ \delta_{IJ} + NxQ_{IJ} + \frac{1}{2}(Nx)^2 (\mathbf{Q}^2)_{IJ} + \dots \right]^{-1} \times \left[ S_{IJ} + \frac{1}{2}Nx (\mathbf{S} \cdot \mathbf{Q} + \mathbf{Q} \cdot \mathbf{S})_{IJ} + \frac{1}{6}(Nx)^2 (\mathbf{S} \cdot \mathbf{Q}^2 + \mathbf{Q} \cdot \mathbf{S} \cdot \mathbf{Q} + \mathbf{Q}^2 \cdot \mathbf{S})_{IJ} + \dots \right]. \quad (4)$$

For the diagonal terms this reduces to

$$\langle \Delta E \rangle_{II} = NxS_{II} + \frac{1}{2}(Nx)^2 (\mathbf{S} \cdot \boldsymbol{\sigma} + \boldsymbol{\sigma} \cdot \mathbf{S})_{II} \dots, \quad (5)$$

where the above definition of  $Q_{IJ}$  has been inserted. For nondiagonal terms one finds

$$\langle \Delta E \rangle_{IJ} = \frac{S_{IJ}}{\sigma_{IJ}} + \frac{1}{2}Nx \frac{1}{\sigma_{IJ}^2} [\sigma_{IJ} (\mathbf{S} \cdot \boldsymbol{\sigma} + \boldsymbol{\sigma} \cdot \mathbf{S})_{IJ} - S_{IJ} (\boldsymbol{\sigma}^2)_{IJ}] \dots. \quad (6)$$

As was to be expected, the slopes in the diagonal terms in the limit of small target thickness determine the fixed-charge stopping cross sections  $S_{II}$ . Nondiagonal terms show a nonzero value in the limit  $x = 0$  which represents the mean energy loss  $\int T d\sigma_{IJ}(T)/\sigma_{IJ}$  in one charge-changing event  $I \rightarrow J$ .

#### B. Thick target

In the opposite case of a thick target, an expansion in terms of eigenvectors of the matrix  $\mathbf{Q}$  may be applied [10],

$$\langle \Delta E \rangle_{IJ} \sim \frac{1}{F_{IJ}^{(0)}} \left[ Nx (\mathbf{F}^{(0)} \cdot \mathbf{S} \cdot \mathbf{F}^{(0)})_{IJ} + \sum' \frac{1}{-q^{(\nu)}} (\mathbf{F}^{(0)} \cdot \mathbf{S} \cdot \mathbf{F}^{(\nu)} + \mathbf{F}^{(\nu)} \cdot \mathbf{S} \cdot \mathbf{F}^{(0)})_{IJ} \right], \quad (9)$$

where  $\sum'$  indicates that the term with the vanishing eigenvalue has been omitted from the sum.

A procedure to carry out sums over eigenvalues without explicit evaluation of eigenvalues and/or eigenvectors involving a characteristic function  $\mathbf{f}(s) = s(s\mathbf{1} - \mathbf{Q})^{-1}$  has been developed in Ref. [10]. In terms of this function, the sum in the brackets of Eq. (9) could be written in the simple form  $d[\mathbf{f}(s) \cdot \mathbf{S} \cdot \mathbf{f}(s)]/ds|_{s=0}$ . Here it is noted that the mean energy loss (9) is made up of three parts,

iting situations will be discussed, a thin target allowing for only a few charge-changing events, and a thick target ensuring charge-state equilibrium. Particular attention will be given to the two-state case.

#### A. Thin target

The case of a thin target is treated by Taylor expansion of the exponential (2) in powers of  $Nx$  with the result

$$F_{IJ}(x) = \sum_{\nu} F_{IJ}^{(\nu)} e^{Nxq^{(\nu)}}, \quad (7)$$

where  $q^{(\nu)}$  is the  $\nu$ th eigenvalue of  $\mathbf{Q}$ ,  $\nu = 0, 1, \dots, n-1$ . The coefficients  $F_{IJ}^{(\nu)}$  can be expressed by eigenvectors, but their explicit form is not needed here. It has been shown that one eigenvalue (numbered  $\nu = 0$ ) always vanishes, and that the real part of all other eigenvalues is nonpositive.  $F_{IJ}^{(0)} \equiv F_J(\infty)$  represents the equilibrium charge-state fraction of state  $J$ . Equations (3) and (7) yield

$$\langle \Delta E \rangle_{IJ} = \frac{1}{F_{IJ}(x)} \sum_{\mu, \nu} (\mathbf{F}^{(\mu)} \cdot \mathbf{S} \cdot \mathbf{F}^{(\nu)})_{IJ} \times \frac{e^{Nxq^{(\mu)}} - e^{Nxq^{(\nu)}}}{q^{(\mu)} - q^{(\nu)}}, \quad (8)$$

where the denominator is given by Eq. (7). The sum splits into a number of terms, several of which decay exponentially with target thickness  $x$  and therefore will be neglected if charge-state equilibrium has been reached at exit. Remaining terms are either proportional to  $x$  or constant. Then,

$$\langle \Delta E \rangle_{IJ} \sim Nx \langle S \rangle + \Delta E_J^{\text{exit}} + \Delta E_I^{\text{entr}}, \quad (10)$$

where  $\langle S \rangle = \sum_K F_K(\infty) S_K$  is the average stopping cross section in charge-state equilibrium and  $S_K = \sum_L S_{KL}$  the stopping cross section involving all transitions from state  $K$ . The intercepts  $\Delta E_J^{\text{exit}}$  and  $\Delta E_I^{\text{entr}}$  depend on the exit and entrance charge state, respectively, and are governed by the final and initial sequences of events.

This separation is meaningful only when the penetrated layer is thick enough so that charge-state equilibrium is reached, as is seen from Fig. 2.

### V. EXAMPLE: THE TWO-STATE CASE

The two-state case may illustrate aspects of more general behavior and has practical importance for light ions in appropriate velocity intervals. The exact expression for the mean energy loss versus thickness is easily determined, yet an appealing form illuminating its physical content has not yet been found. In the limit of small thickness, Eqs. (5) and (6) yield

$$\langle \Delta E \rangle_{11} = NxS_{11} + \frac{1}{2}(Nx)^2 (\sigma_{12}S_{21} + \sigma_{21}S_{12}) \cdots, \quad (11)$$

where terms of third and higher order in  $Nx$  have been omitted, and

$$\begin{aligned} \langle \Delta E \rangle_{12} = & \frac{S_{12}}{\sigma_{12}} + \frac{1}{2}Nx(S_{11} + S_{22}) \\ & + \frac{1}{6}(Nx)^2 (\sigma_{12}S_{21} + \sigma_{21}S_{12}) \\ & + \frac{1}{12}(Nx)^2 (\sigma_{21} - \sigma_{12})(S_{11} - S_{22}) \cdots, \quad (12) \end{aligned}$$

whereas  $\langle \Delta E \rangle_{21}$  and  $\langle \Delta E \rangle_{22}$  can be obtained by interchanging indices.

The first term in Eq. (11) reflects the fixed-charge stopping power, and the second term is nonvanishing only if charge-changing events contribute noticeably to the energy loss. Whether or not they do can be decided if experimental data allow one to distinguish between a second- and a third-order dependence on depth.

The first term in Eq. (12) represents the mean energy transfer in one charge-changing event. It shows up as an intercept that can be identified directly [6]. The second term reflects a straight average between the two fixed-charge stopping powers. Indeed, the location of the one allowed charge-changing event (in the first order in  $Nx$ ) is distributed uniformly across the layer. The third term is similar but not identical to the second term in (11), and the fourth term hinges on the difference between the fixed-charge stopping cross sections as well as the capture and loss cross section.

The theoretical description presented in Ref. [6] allows for one charge-changing event only and is, therefore, valid up to the term linear in  $Nx$ . It is easily verified that of the two quadratic terms in (12), the first is ignored in that description while the second is recovered.

In the thick-layer limit, the terms entering into Eq. (10) reduce to  $\langle S \rangle = (\sigma_{21}S_1 + \sigma_{12}S_2)/\sigma$  for the average stopping cross section, where  $\sigma = \sigma_{12} + \sigma_{21}$  and

$$\Delta E_1^{\text{entr}} = \frac{\sigma_{12}}{\sigma^2}(S_1 - S_2), \quad (13)$$

$$\Delta E_1^{\text{exit}} = \frac{\sigma_{12}}{\sigma^2}(S_1 - S_2) + \frac{1}{\sigma\sigma_{21}}(\sigma_{12}S_{21} - \sigma_{21}S_{12}),$$

whereas the terms for  $I$  and  $J = 2$  may be obtained by interchanging indices.

### VI. SUM RULES

The two relationships Eq. (13) and their counterparts for  $1 \leftrightarrow 2$  are not independent. Indeed,  $\sigma_{21}\Delta E_1 + \sigma_{12}\Delta E_2 = 0$  for both entrance and exit. These are special cases of the sum rules

$$\sum_I F_I(\infty)\Delta E_I^{\text{exit}} = 0, \quad \sum_J F_J(\infty)\Delta E_J^{\text{entr}} = 0. \quad (14)$$

Here, the first relation follows from the fact that if the spectrum is summed over all exit states, the intercept can only depend on the entrance state [10]. The second relation represents the fact that no intercept can occur upon entrance if the initial beam is already in charge-state equilibrium. Both relations follow from Eqs. (9) and (10). Moreover, sum rules involving the measured intercepts  $\epsilon_{IJ} = \Delta E_I^{\text{entr}} + \Delta E_J^{\text{exit}}$  emerge directly from separability. For the two-state case,  $\epsilon_{11} - \epsilon_{12} = \epsilon_{21} - \epsilon_{22}$ .

### VII. ANALYSIS OF EXPERIMENTAL DATA

In the discussion of strategies for analyzing experimental data, possible post-foil changes in charge-state population and associated energy-loss processes will be ignored. If necessary, such processes can be incorporated by convolution of two distributions of the type of Eq. (1), one for the foil and one for the flight path between foil and detector.

Analysis in the low-thickness limit is evidently to be preferred, because all pertinent cross sections can be extracted from the limiting behavior of charge-state populations and mean energy losses. Taking into account quadratic terms in  $Nx$  may overdetermine the system of available equations and thus allow one to optimize extracted parameters.

The data reported in Ref. [6] cover a wide enough range of foil thickness to allow data analysis both in the low- and high-thickness limit. While the importance of both  $S_{12}$  and  $S_{21}$  is readily verified from inspection of the low-thickness behavior, the same conclusion can also be deduced from the asymptotic behavior alone.

In the frequent situation where measurements in the low-thickness limit are impossible for experimental reasons, the present analysis suggests a procedure based on charge-state equilibrium, as was stipulated on qualitative grounds in Sec. II.

Consider  $n$  significant states.

(a) Experimentally accessible information includes  $n$  equilibrium charge-state populations, i.e.,  $n - 1$  independent parameters since they must add up to 1; then there is the equilibrium stopping power; finally, there are  $n \times n$  intercepts which reduce to  $2n - 2$  independent parameters. This yields a total of  $3n - 2$  independent measurable quantities.

(b) Next, consider the number of atomic parameters which one would like to determine. In principle, there

are  $n^2$  stopping cross sections and  $n^2 - n$  charge-exchange cross sections, which exceeds the number of measurable parameters for all  $n \geq 2$ . This, however, includes a large number of quantities that are exceedingly small or even vanishing, such as the cross section for capture of 92 electrons by a  $U^{92+}$  projectile ion in one collision with a target atom. A more realistic set of nonvanishing parameters includes the  $n$  diagonal elements of the stopping matrix  $\mathbf{S}$  — implying that all energy loss in charge-changing collisions is negligible [7,8,11,12] — and the  $2(n-1)$  capture and loss cross sections for one-electron processes. This adds up to  $3n - 2$  parameters which is just what can be measured.

This ignores any use of theoretically predicted atomic parameters. The above extraction scheme may be improved if even only rough data — theoretical or experimental — are available on the energy loss in charge-changing events or the significance of two-electron processes. A consistency check may be gained from straggling measurements:

Charge-exchange straggling is governed by  $\sigma_{IJ}$  and  $S_{IJ}$  only [10,11], i.e., the same parameters that determine transients in stopping power. Thus, even from measurements in charge-state equilibrium it should be possible to determine charge-exchange cross sections in solids and to avoid postulating scaling rules for fixed-charge stopping cross sections (like the common  $q^2$  relation) that ought to be the result of a measurement or a theoretical model [12,13].

#### ACKNOWLEDGMENTS

The author would like to thank Professor Y. Le Beyec and his colleagues for their hospitality at IPN Orsay and for stimulating this study. This work has been supported by the Centre National de la Recherche Scientifique (CNRS) and the Danish Natural Science Research Council (SNF).

- 
- [1] G. H. Henderson, Proc. R. Soc. London Ser. A **102**, 496 (1922).
  - [2] S. K. Allison, J. Cuevas, and M. Garcia-Munos, Phys. Rev. **127**, 792 (1962); J. Cuevas, M. Garcia-Munos, P. Torres, and S. K. Allison, *ibid.* **135**, A335 (1962); M. N. Hubermann, *ibid.* **127**, 799 (1962).
  - [3] S. Datz, J. Gomez del Campo, P. F. Dittner, P. D. Miller, and J. A. Biggerstaff, Phys. Rev. Lett. **38**, 1145 (1977).
  - [4] J. A. Golovchenko, A. N. Goland, J. S. Rosner, C. E. Thorn, H. E. Wegner, H. Knudsen, and C. D. Moak, Phys. Rev. B **23**, 957 (1981).
  - [5] N. E. B. Cowern, P. M. Read, C. J. Sofield, L. B. Bridwell, and M. W. Lucas, Phys. Rev. A **30**, 1682 (1984); N. E. B. Cowern, P. M. Read, C. J. Sofield, L. B. Bridwell, G. Huxtable, M. Miller, and M. W. Lucas, Nucl. Instrum. Methods **2**, 112 (1984); N. E. B. Cowern, P. M. Read, and C. J. Sofield, *ibid.* **12**, 43 (1985); L. B. Bridwell, N. E. B. Cowern, P. M. Read, and C. J. Sofield, *ibid.* **13**, 123 (1986).
  - [6] H. Ogawa, I. Katayama, H. Ikegami, Y. Haruyama, A. Aoki, M. Tosaki, F. Fukuzawa, K. Yoshida, I. Sugai, and T. Kaneko, Phys. Rev. B **43**, 11370 (1991); H. Ogawa, I. Katayama, H. Ikegami, Y. Haruyama, A. Aoki, M. Tosaki, F. Fukuzawa, K. Yoshida, and I. Sugai, Phys. Lett. A **160**, 77 (1991); H. Ogawa, I. Katayama, I. Sugai, Y. Haruyama, A. Aoki, M. Tosaki, F. Fukuzawa, K. Yoshida, and H. Ikegami, Nucl. Instrum. Methods **69**, 108 (1992).
  - [7] K. B. Winterbon, Nucl. Instrum. Methods **144**, 311 (1977).
  - [8] T. Kaneko and Y. Yamamura, Phys. Lett. A **100**, 313 (1984).
  - [9] P. Sigmund, in *Interaction of Charged Particles with Solids and Surfaces*, edited by A. Gras-Martí *et al.*, Vol. 271 of *NATO Advanced Study Institute Series B: Physics* (Plenum, New York, 1991), p. 73.
  - [10] P. Sigmund, Nucl. Instrum. Methods B **69**, 113 (1992).
  - [11] O. Vollmer, Nucl. Instrum. Methods **121**, 373 (1974).
  - [12] A. Arnau, M. Peñalba, and P. M. Echenique, F. Flores, and R. H. Ritchie, Phys. Rev. Lett. **65**, 1024 (1990); A. Arnau, M. Peñalba, and P. M. Echenique, Nucl. Instrum. Methods B **69**, 102 (1992).
  - [13] W. Brandt and M. Kitagawa, Phys. Rev. B **25**, 5631 (1982).